INTERACTION OF LASER RADIATION WITH MATTER

PACS numbers: 52.50.Jm; 52.57.Bs; 52.38.Ph
DOI: 10.1070/QE2001v031n12ABEH002104

X-ray spectral measurement of high-temperature plasma parameters in porous targets irradiated with high-power laser pulses

V V Gavrilov, A Yu Gol'tsov, N G Koval'skii, S N Koptyaev, A I Magunov, T A Pikuz, I Yu Skobelev, A Ya Faenov

***Abstract*. The X-ray spectra of multiply charged ions were recorded from planar agar $(C_{12}H_{18}O_9)_n$ based targets with an average density of 2 mg cm^{-3} irradiated by high-power laser pulses ($\lambda = 1.054$ μm, $\tau = 2.5$ ns, $I \approx 5 \times 10^{13}$ W cm^{-2}). The spectra were recorded with a high spectral and spatial resolution employing spherically bent (focusing) crystals of mica and quartz. An analysis of the experimental data obtained by the irradiation of Al_2O_3-doped agar samples allowed us to determine the main parameters of the plasma produced inside the targets. The ion temperature of plasma in low-density porous targets was estimated for the first time to be 1.5 – 2 times higher than the electron temperature.**

Keywords: *high-power laser radiation, high-temperature plasma, X-ray spectral lines of multiply charged ions, low-density porous medium, X-ray crystal spectrograph.*

1. Introduction

The investigation of physical processes occurring in plasmas produced upon the interaction of high-intensity (10^{13} – 10^{14} W cm^{-2}) laser radiation with low-density (1 – 100 mg cm^{-3}) porous materials is of great interest for some promising fields of basic scientific research such as inertial confinement fusion (ICF), the physics of high-energy densities, and the laboratory simulation of astrophysical phenomena. At the present-day stage of ICF research program the key problem is the target design matching to laser pulse parameters and irradiation conditions. One of the promising approaches is the target design optimisation by using volume-structured low-density materials (for instance, in order to provide the efficient smoothing of laser irradiation nonuniformities and ensure the stable compression of fusion targets [1, 2]). Porous media doped with heavy elements are currently actively investigated in the search for the ways to control the spectrum of X-rays emitted by the plasma [3].

In this paper, we present the results of experiments performed on the 'Mishen' facility, which are a continuation of the earlier studies of the laser – porous media interaction [4 – 8]. The aim of our work is to obtain a more detailed information on the plasma produced inside laser-irradiated porous samples.

2. Experimental

The experiments were performed on the 'Mishen' facility [9] in the 'Troitsk Institute of Innovation and Fusion Research' State Scientific Centre. The facility had the following parameters: a laser radiation wavelength of 1.054 μm, 2.5-ns laser pulse with energy up to 100 J; and the energy contrast ratio of no less than 10^6. The laser beam was focused on a target with a lens of 1:16 aperture ratio; the average power density was $\sim 5 \times 10^{13}$ W cm^{-2} over the focal spot of $\sim$ 250 μm in diameter on the target surface. Planar 300 – 500-μm thick targets fabricated on the base of agar $(C_{12}H_{18}O_9)_n$ with a density of 1 mg cm^{-3} were placed in a vacuum interaction chamber. Fine-dispersed Al_2O_3 powder (with microparticle diameters of less than 1 μm) was introduced into the agar samples as an admixture with the same average density. The agar samples used in the experiments had a chaotic structure of solid-density fibrous 1 – 2 μm in diameter spaced at 10 – 50 μm. In some experiments the 6-μm thick aluminium foils were also used as the targets.

The X-ray plasma radiation was analysed using four spectrographs with spherically bent (focusing) crystals of mica and quartz [10 – 12], which provided a high spectral resolution ($\lambda/\Delta\lambda \geqslant 5000$) and a high spatial resolution of $\sim 20 - 30$ μm. The spectra of aluminium ions were recorded in the second diffraction order by three mica spectrographs and in the first order by the quartz spectrograph. The mica spectrographs recorded the He_β line of Al XII ions ($\lambda \sim 6.63$ Å), the He_γ line of Al XII ($\lambda \sim 6.31$ Å), and the Ly_α line of Al XIIII ($\lambda \sim 7.17$ Å), while the quartz spectrograph recorded the He_α line of Al XII ($\lambda \sim 7.76$ Å). Note that the high sensitivity of the focusing spectrographs allowed us to obtain the aluminium ion spectra in a single laser shot.

V V Gavrilov, A Yu Gol'tsov, N G Koval'skii, S N Koptyaev 'Troitsk Institute for Innovation and Fusion Research' State Research Center, 142190 Troitsk, Moscow Oblast, Russia; e-mail: vvgavril@triniti.ru; fax: 7 (095) 334 50 56; 7 (095) 334 56 67;
A I Magunov, T A Pikuz, I Yu Skobelev, A Ya Faenov All-Russian Scientific Research Institute of Physicotechnical and Radio Engineering Measurements, 141570 Mendeleevo, Moscow Oblast, Russia

Received 18 July 2001
Kvantovaya Elektronika **31** (12) 1071 – 1074 (2001)
Translated by E N Ragozin

To control the focal spot dimensions, an X-ray pinhole camera was used.

3. Experimental results and discussion

It was shown earlier [4–8] that upon irradiation of a porous medium, laser light is absorbed inside the low-density samples, and a high-temperature plasma layer is produced inside the porous target. For a target with the initial density of 2 mg cm^{-3}, the depth of this layer was 300–400 μm (in the direction of laser beam propagation). For targets with the initial density of 10 mg cm^{-3}, the layer depth was equal to 100–150 μm only. In the direction perpendicular to the laser beam, the dimension of the hot plasma region inside the porous target was somewhat larger than the focal spot diameter and slightly depended on the agar density.

The X-ray pulse duration recorded with vacuum diodes and an X-ray streak camera was 3–4 ns, i.e., was nearly equal to the laser pulse duration. The plasma electron temperature T_e was determined by processing X-ray images obtained with filtered pinhole cameras. For porous targets with the density of 2 mg cm^{-3}, it was 0.8–1 keV near the centre of the extended plasma region and decreased somewhat to 0.6–0.7 keV deep into the target.

In this work, we obtained spectra of multiply charged aluminium ions with a spatial resolution along the normal to the target surface in experiments on laser irradiation of agar samples with the average density of 1 mg cm^{-3} doped with Al_2O_3 of 1 mg cm^{-3} average density too. The examples of spectrograms are presented in Fig. 1. The longitudinal depth of the emission region inside the low-density targets was equal to 0.35–0.4 mm for all the lines recorded.

Quite unexpectedly, we observed in our experiments the spectra of sulphur and chlorine multiply charged ions (Fig. 1). These dopants are probably introduced in the process of agar sample fabrication. As shown below, the existence of sulphur and chlorine dopants turned out to be very useful for solving some problems encountered in the study.

The main results were supposed to be obtained from the analysis of the Al XII ion spectrum [the resonance line $He_{\alpha1}$ (R), the intercombination line $He_{\alpha2}$ (I), and the satellites (k, j)]. We planned to determine the plasma temperature and density from the intensity ratios $I_{k,j}/I_R$ and I_R/I_I, respectively. However, the high intensity of the resonance line I_R resulted in the overexposure of the recording X-ray photographic film, and the above approach could not be realised.

Generally speaking, the plasma density could be determined from the intensity ratio $I_{k,j}/I_I$, however, this ratio depends not only on the density but on the temperature as well. This fact implies that the He_α spectrum of the Mg XII ion could be used for the density determination only in combination with independent measurements of the plasma temperature.

We managed to estimate the plasma temperature due to the presence of sulphur and chlorine dopants in the porous target. Fig. 2 shows the relative intensities of the He_α line spectrum of the S XV ion recorded with the mica crystal in the third diffraction order. The line intensity ratio $I_{k,j}/I_R$ from this spectrogram resulted in $T_e = 800$ eV. This temperature value and the line intensity ratio $I_{k,j}/I_I$ for the Al XII ion give the plasma density $N_e = 6 \times 10^{20}$ cm^{-3}.

The spectra also contained the information on the spatial distribution of the plasma parameters in the emission region. By measuring the line intensity ratio $I_{k,j}/I_R$ we

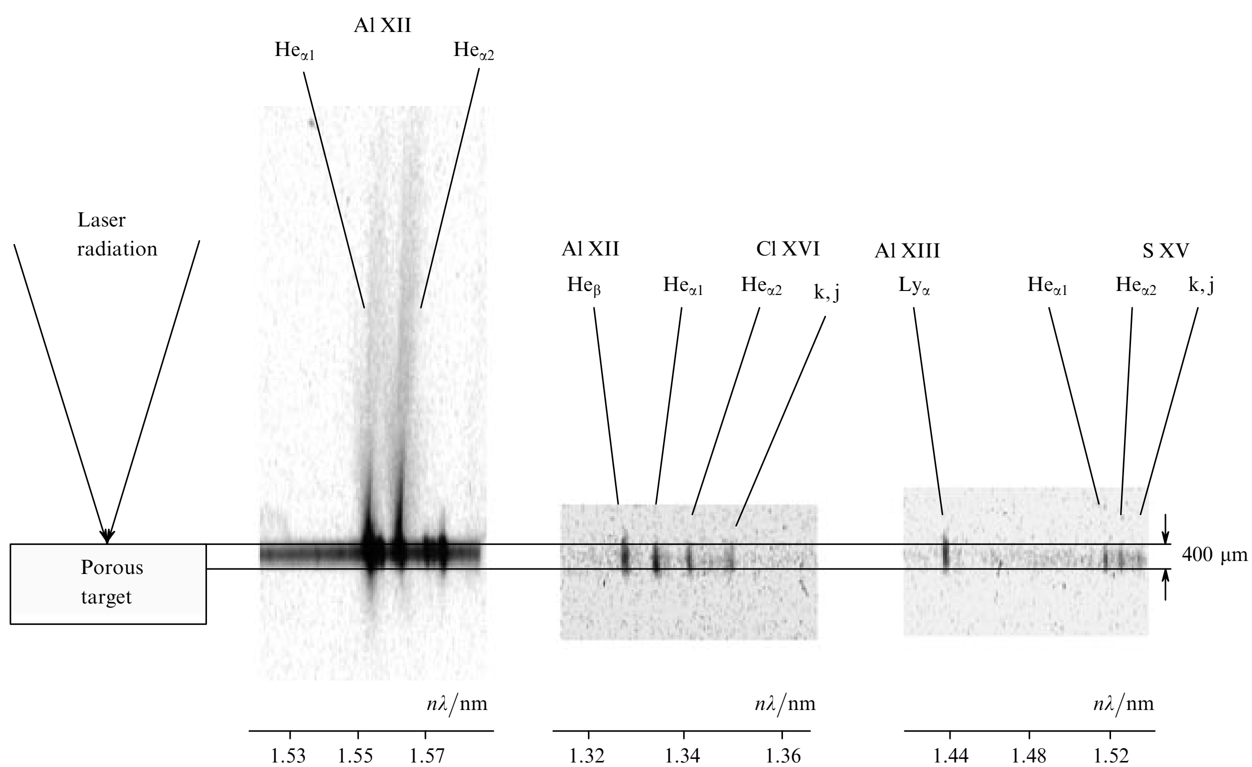

Figure 1. Spectrograms of line emission of Al XII, Al XIII, Cl XVI, and S XV ions recorded with the mica spectrograph upon laser irradiation of Al_2O_3-doped agar samples ($n = 2$ for the lines of aluminium ions and $n = 3$ for the lines of chlorine and sulphur ions).

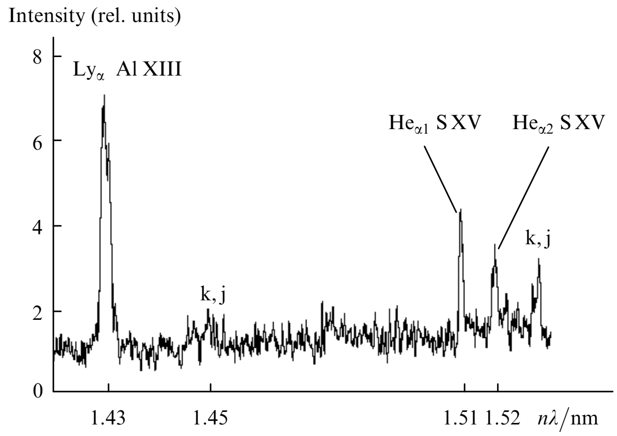

Figure 2. Relative intensities of the Al XIII line emission recorded in the second diffraction order and of the S XV line emission recorded in the third difraction order.

determined the electron plasma temperature in different regions inside the porous sample, which was 750, 800, and 650 eV at distances of 190, 220, and 250 μm from the target surface, respectively. Unfortunately, we failed to measure reliably the spatial distribution of the plasma density from the Al XII ion lines because the accuracy of T_e measurements was insufficient due to the low intensity of chlorine spectral lines. The plasma parameters presented in Table 1 are related to the region located inside the porous sample at a distance of $\sim$ 220 μm from the target surface.

Table 1. Plasma parameters determined by different diagnostic techniques.

Ion	Line intensity ratios used in the work	N_e/cm^{-3}	T_e/eV
Cl XVI	R/I	$< 10^{21}$	–
S XV	R/I	$< 10^{21}$	–
Cl XVI	k, j/R	–	650 – 800
S XV	k, j/R	–	600 – 800
Al XII	k, j/I	6×10^{20}	–

We also estimated from the spectra another very important parameter – the plasma ion temperature. The ion temperature was determined from the Doppler broadening of the spectral lines. For the 2 – 1 transitions in the He-like Cl XVI ion at an electron density below 10^{21} cm^{-3}, the Stark broadening is known to be very small. Because of the low chlorine density in the target, the optical thickness of the plasma is less than unity even for the resonance line. Under these conditions, the line width is determined only by the ion motion.

Note that the stage of plasma formation (evaporation of individual structural elements of the porous medium and the filling of the pores by hydrodynamic plasma flows) lasted only 0.2 – 0.3 ns under our experimental conditions [4], whereas the laser pulse duration was 2.5 ns. Therefore, the contribution from the macroscopic plasma flows to the Doppler broadening can be neglected in the time-integrated spectra obtained, and the ion plasma temperature can be evaluated from the widths of spectral lines.

The relative full width at half maximum (FWHM) of the Cl XVI intercombination line is $\Delta\lambda/\lambda = 4.9 \times 10^{-4}$ (Fig. 3), which gives $T_i \approx 1.4$ keV, i.e., the ion plasma temperature is 1.5 – 2 times higher than the electron temperature. Note that a significant excess of the ion temperature over the electron temperature in a plasma produced by high-power laser irradiation of low-density porous targets was theoretically predicted in papers [13, 14], where the production of the nonequilibrium plasma in a porous medium was analysed in detail.

Thus, we have estimated for the first time the ion temperature in a plasma generated by the laser irradiation of targets made of porous materials. Under our experimental conditions, the ion temperature was approximately two times higher than the electron temperature.

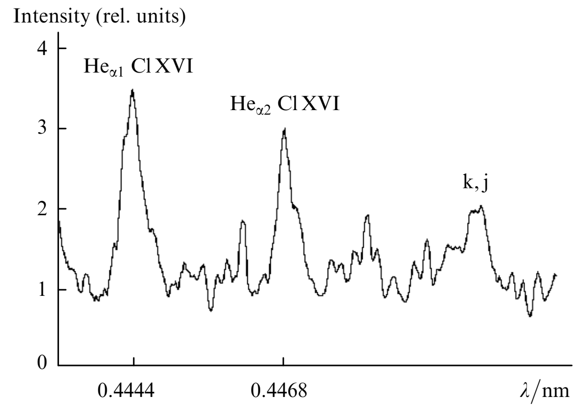

Figure 3. Relative intensities of the Cl XVI ion line spectrum emitting from the interior region of a low-density sample spaced at $\sim$ 220 μm from the surface under irradiation.

Acknowledgements. This work was supported by the Russian Foundation for Basic Research (Grants Nos 01-02-17336 and 01-02-17361). The authors thank S F Medovshchikov for the fabrication of porous targets and A E Bugrov, I N Burdonskii, E V Zhukalo, V N Kondrashov, V G Nikolaevskii, and V M Petryakov for their assistance in the performance of experiments.

References

1. Gus'kov S Yu, Zmitrenko N V, Rozanov V B *Zh. Eksp. Teor. Fiz.* **108** 548 (1995) [*JETP* **81** 296 (1995)]
2. Desselbeger M, Jones M W, Edwards J, et al. *Phys. Rev. Lett.* **74** 2961 (1995)
3. Lindl J *Phys. Plasmas* **2** 3933 (1995)
4. Bugrov A E, Burdonskii I N, Gavrilov V V, et al. *Zh. Eksp. Teor. Fiz.* **111** 903 (1997) [*JETP* **84** 407 (1997)]
5. Burdonsky I N, Bugrov A E, Gavrilov V V, et al. *Rev. Sci. Instrum.* **68** 810 (1997)
6. Bugrov A E, Burdonskii I N, Gavrilov V V, et al. *Zh. Eksp. Teor. Fiz.* **115** 805 (1999) [*JETP* **88** 441 (1991)]
7. Bugrov A E, Burdonsky I N, Gavrilov V V, et al. *Laser Part. Beams* **17** 415 (1999)
8. Bugrov A E, Burdonsky I N, Gavrilov V V, et al., in *Inertial Fusion Sciences and Applications* Ch Labaune, Hogan W, and Tanaka K A (Eds) (Paris: Elsevier, 2000) p.355
9. Bolotin V A, Burdonsky I N, Gavrilov V V, et al. *Rev. Sci. Instrum.* **61** 3259 (1991)
10. Bryunetkin B A, Pikuz S A, Skobelev I Yu, et al. *Laser Part. Beams* **10** 849 (1992)
11. Faenov A Ya, Agafonov Yu A, Bryunetkin B A, et al. *Proc. SPIE Int. Soc. Opt. Eng.* 2015 64 (1993)

12. Bryunetkin B A, et al. *Kvantovaya Elektron*. **21** 142 (1994) [*Quantum Electron*. **24** 133 (1994)]
13. Gus'kov S Yu, Rozanov V B *Kvantovaya Elektron*. **24** 715 (1997) [*Quantum Electron*. **27** 696 (1997)]
14. Gus'kov S Yu, Zmitrenko N V, Rozanov V B *Pis'ma Zh. Eksp. Teor. Fiz*. **66** 521 (1997)